LA-UR-18-20858
Approved for public release; distribution is unlimited.

Title: Pre-inverted SESAME data table construction enhancements to correct unexpected inverse interpolation pathologies in EOSPAC 6

Author(s): Pimentel, David A.
Sheppard, Daniel Glen

Intended for: Report

Issued: 2018-02-07 (rev.1)

Pre-inverted SESAME data table construction enhancements to correct unexpected inverse interpolation pathologies in EOSPAC 6

David A. Pimentel[1] and Daniel G. Sheppard[2]

[1]WRS-SNA, Los Alamos National Laboratory, *davidp@lanl.gov*
[2]XCP-5, Los Alamos National Laboratory, *danielsheppard@lanl.gov*

February 1, 2018

Abstract

It was recently demonstrated that EOSPAC 6 continued to incorrectly create and interpolate pre-inverted SESAME data tables after the release of version 6.3.2beta.2. Significant interpolation pathologies were discovered to occur when EOSPAC 6's host software enabled pre-inversion with the *EOS_INVERT_AT_SETUP* option. This document describes a solution that uses data transformations found in EOSPAC 5 and its predecessors. The numerical results and performance characteristics of both the default and pre-inverted interpolation modes in both EOSPAC 6.3.2beta.2 and the fixed logic of EOSPAC 6.4.0beta.1 are presented herein, and the latter software release is shown to produce significantly-improved numerical results for the pre-inverted interpolation mode.

I. Introduction

EOSPAC 6's [1] interpolation of inverted SESAME [2] data has been shown to be a problem when pre-inversion of SESAME data tables is enabled with the *EOS_INVERT_AT_SETUP* option[1]. In previous discussions [3][4], it was concluded that unwanted numerical errors, which were observed during the interpolation of inverted SESAME data, manifested as a result of tabular edge effects. Unfortunately, it was later discovered that that conclusion was either incomplete or naïve.

All interpolation in this investigation was performed using EOSPAC 6's birational interpolator, which corresponds to the default *EOS_RATIONAL* option and was derived from previous work [5].

II. Background

A. Symbols and Syntax

The symbols and mnemonics used in this document, which correspond to those described within the EOSPAC 6 user manual [1], are listed in tables 1 and 2.

[1]The *EOS_INVERT_AT_SETUP* option is enabled during the EOSPAC 6 setup phase

Table 1: EOSPAC 6 and general symbols and descriptions.

SYMBOL		
EOSPAC 6	GENERAL	DESCRIPTION
EOS_T_DUt	$T(\rho, Ut)$	Temperature (Density- and Total Specific-Internal-Energy-dependent)
EOS_T_DPt	$T(\rho, Pt)$	Temperature (Density- and Total Pressure-dependent)
EOS_Pt_DUt	$Pt(\rho, Ut)$	Total Pressure (Density- and Total Specific-Internal-Energy-dependent)
EOS_Ut_DPt	$Ut(\rho, Pt)$	Total Specific-Internal-Energy (Density- and Total Pressure-dependent)
EOS_D_PtT	$\rho(Pt, T)$	Density (Total Pressure- and Temperature-dependent)

Table 2: Indvidual mnemonic descriptions.

SYMBOL	DESCRIPTION
Ut	Total specific internal energy
Pt	Total pressure
U^*	Transformed specific internal energy
P^*	Transformed pressure
ρ or D	Density
T	Temperature
$Uc(\rho)$	Cold curve specific internal energy *i.e.*, $Ut(\rho, T = 0)$
$Pc(\rho)$	Cold curve pressure *i.e.*, $Pt(\rho, T = 0)$
f and g	General symbols used herein to represent arbitrary tabulated functions
v	Mass-specific volume

B. Table Inversion

One may wonder what is meant by the term "inversion" and its various forms (i.e., inverted, pre-inverted, default inversion, etc.), when it is used in reference to SESAME data. In general, SESAME data are tabulated representations of equilibrium material properties — specifically equation of state (EOS) in the context of this discussion — that are often bivariate functions of density and temperature: $f(\rho, T)$. The "inversion" of such a table is the data transformation required to exchange the dependent variable data with one of the independent variables. For example, $f(\rho, T)$ can be transformed into a new tabulated representation as follows: $T(\rho, f)$ or $\rho(f, T)$. An extension of this transformation uses two SESAME tables, $f(\rho, T)$ and $g(\rho, T)$, to produce a new tabulated representation as follows: $f(\rho, g)$, $g(\rho, f)$, $f(g, T)$, or $g(f, T)$. For example, $f(\rho, T)$ and $g(\rho, T)$ can be transformed into $f(\rho, g)$ first by inverting $g(\rho, T)$ $\rightarrow$ $T(\rho, g)$ and merging with $f(\rho, T)$ to yield $f(\rho, g)$. Of course, such generalizations are not always feasible; consequently, EOSPAC 6 limits the available transformation combinations [1, Appendix B].

C. Inverse Interpolation Modes

EOSPAC 6 currently provides two general interpolation modes: the default and pre-inverted. The default interpolation mode has existed for the entire life of EOSPAC 6, and it is dependent upon loading SESAME data into memory with the same dependent and independent variables as are stored in the SESAME data files: $f(\rho, T)$. The interpolation phase of operation is then required to converge on inverse solutions (i.e., $T(\rho, f), \rho(f, T), etc.$) using its iterative algorithms. Needless to say, this default mode has proven to be too slow for large scale problems that are simulated by various host software.

Alternatively, the pre-inverted interpolation mode is a recent feature of EOSPAC 6, and it is based upon the notion that an inverted table is created during the setup phase of operation and stored in memory. Such inverted tables are subsequently used directly, and no iterative algorithms are required during EOSPAC 6's interpolation phase of operation. This is proven to significantly-improve interpolation performance, and the various host software simulations benefit from the boost. Automatically defining the new inverse table grid and populating the new inverted table is where this scheme is difficult to implement so that the interpolated results are numerically comparable to those generated by the default interpolation mode.

D. Data

The original test case was provided by an EOSPAC 6 user, and it was based upon the EOS test trajectory that is shown in figure 1 (page 4). The test trajectory consisted of 1201 triplets – each containing a density, a pressure, and an internal energy value. When the defined trajectory was used as input for EOSPAC 6's default inverse interpolation mode, the interpolated results for the aluminum EOS numbered 3720 [6] were produced as two temperature traces shown as the solid black curves in figures 2 and 3 (pages 4 and 5). Unfortunately, when the same trajectory was used as input for EOSPAC 6's pre-inverted interpolation mode, the interpolated results were produced as two temperature traces shown as the solid black curves in figures 4 and 5 (pages 5 and 6).

The oscillatory inverse interpolation results shown in figures 4 and 5 demonstrate a pathology that was assumed to be resolved in the previous discussions [3][4].

III. Discussion

A. Baseline Data

The aforementioned interpolation pathologies were unexpected, and they pressed the authors to further investigate the inverse interpolation behavior over a significantly larger range of inputs. Figures 6 and 7 (pages 6 and 7) show logarithmically-spaced, interpolated isobars superimposed on the representative SESAME data for both the default and pre-inverted inverse interpolation modes respectively. The inverse interpolation pathologies are demonstrated to affect large ranges of interpolator inputs – especially near the edges of the inverted SESAME data table (figure 7). Notice that the oscillatory pre-inverted interpolated isobaric lines (gray) shown in figures 7 and 8 (pages 5 and 6) reiterate the demonstrated numerical pathology previously-identified by the interpolated curves (black) of figures 4 and 5.

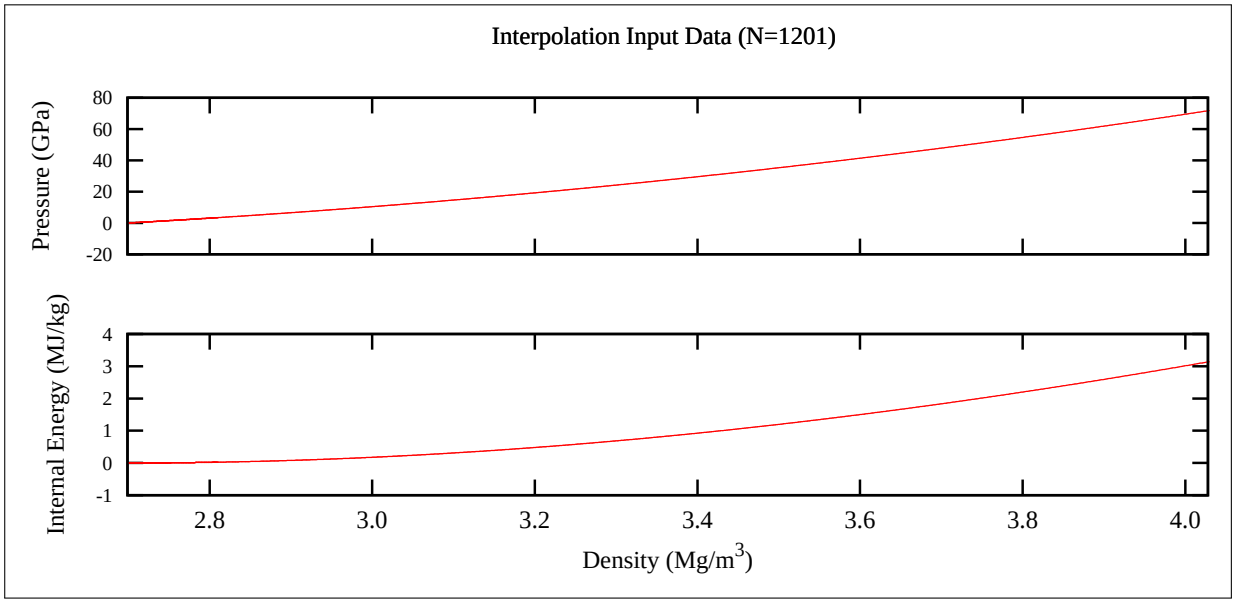

Figure 1: Equation of state test trajectory.

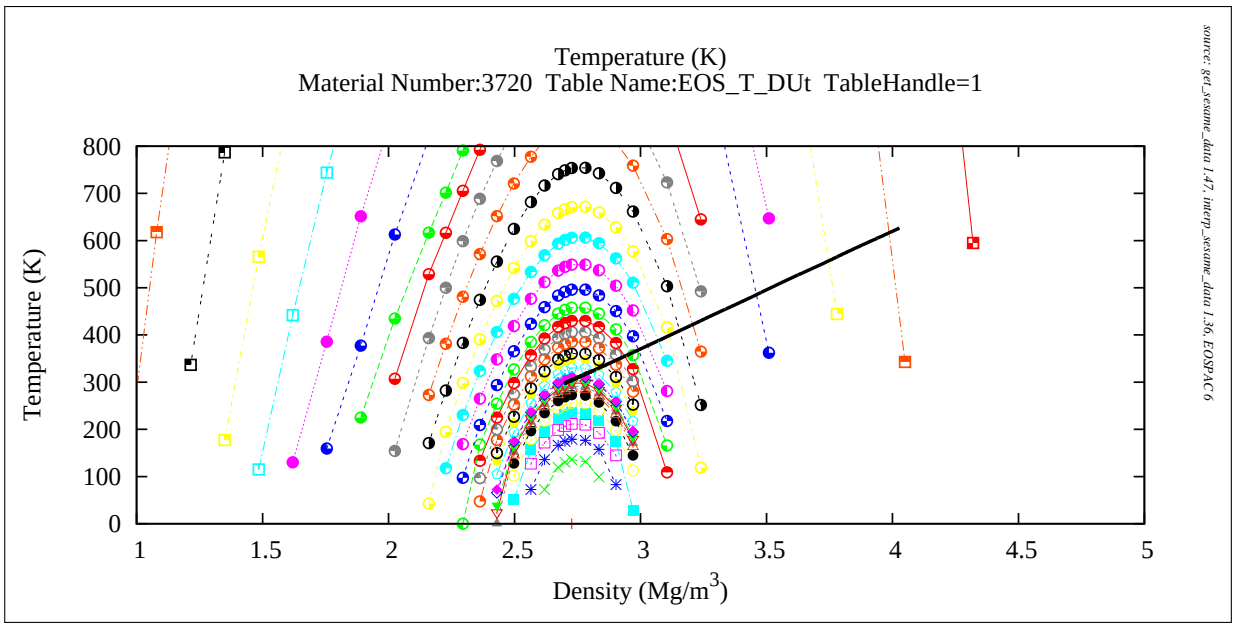

Figure 2: Interpolated $T(\rho, Ut)$ trajectory (black curve), which was calculated using EOSPAC 6's default inverse interpolation mode, superimposed on the representative iso-energy lines of SESAME data.

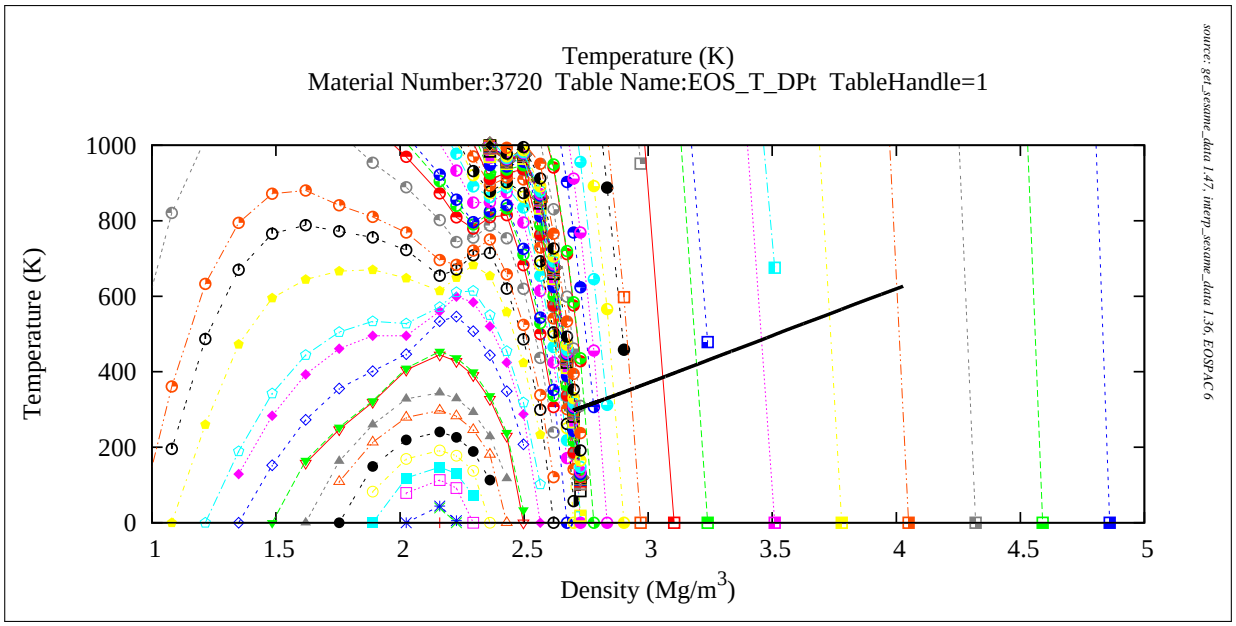

Figure 3: Interpolated $T(\rho, Pt)$ trajectory (black curve), which was calculated using EOSPAC 6's default inverse interpolation mode, superimposed on the representative isobaric lines of SESAME data.

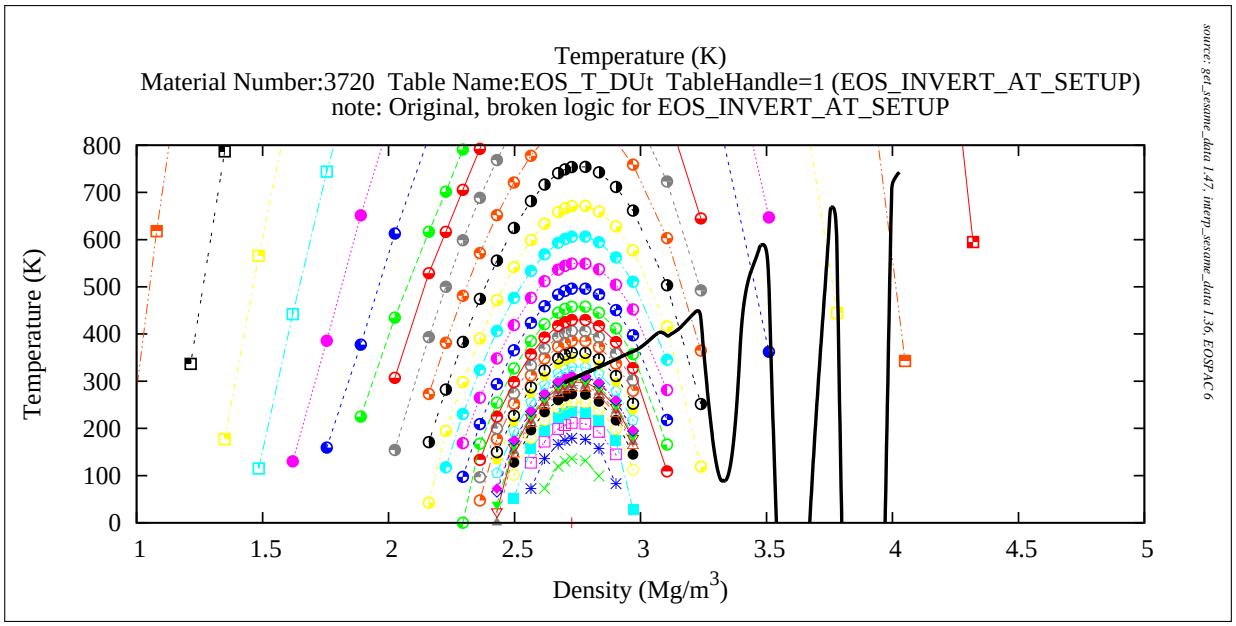

Figure 4: Interpolated $T(\rho, Ut)$ trajectory (black curve), which was calculated using EOSPAC 6's pre-inverted (i.e., *EOS_INVERT_AT_SETUP*) inverse interpolation mode, superimposed on the representative iso-energy lines of SESAME data.

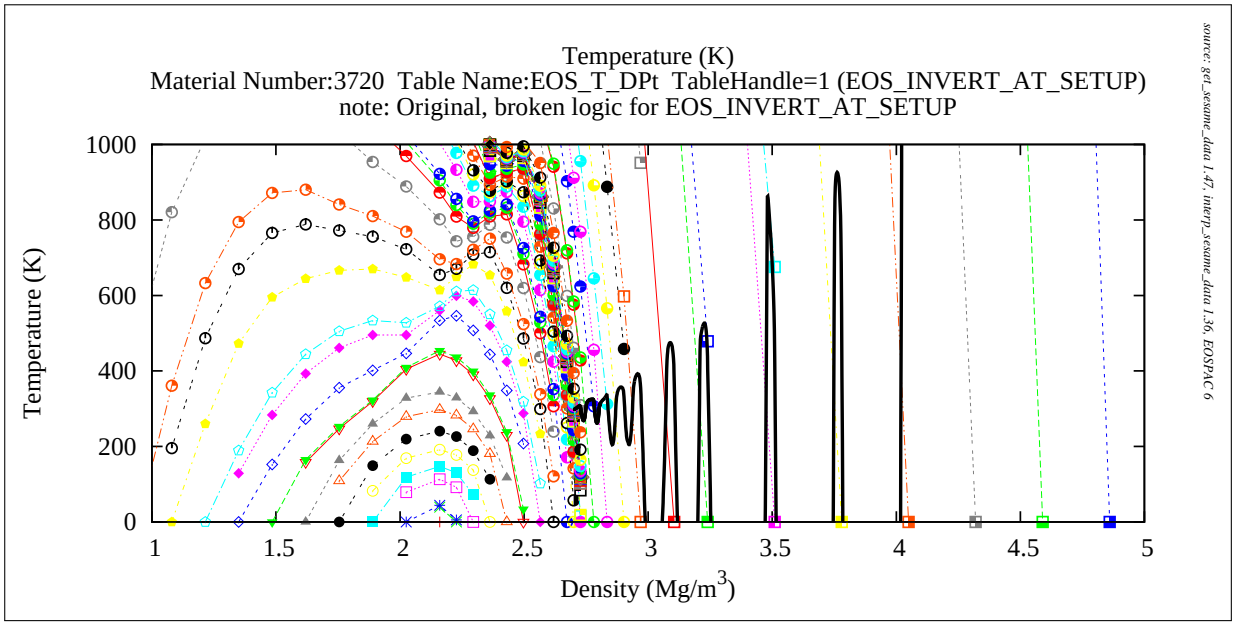

Figure 5: Interpolated $T(\rho, Pt)$ trajectory (black curve), which was calculated using EOSPAC 6's pre-inverted (i.e., *EOS_INVERT_AT_SETUP*) inverse interpolation mode, superimposed on the representative isobaric lines of SESAME data.

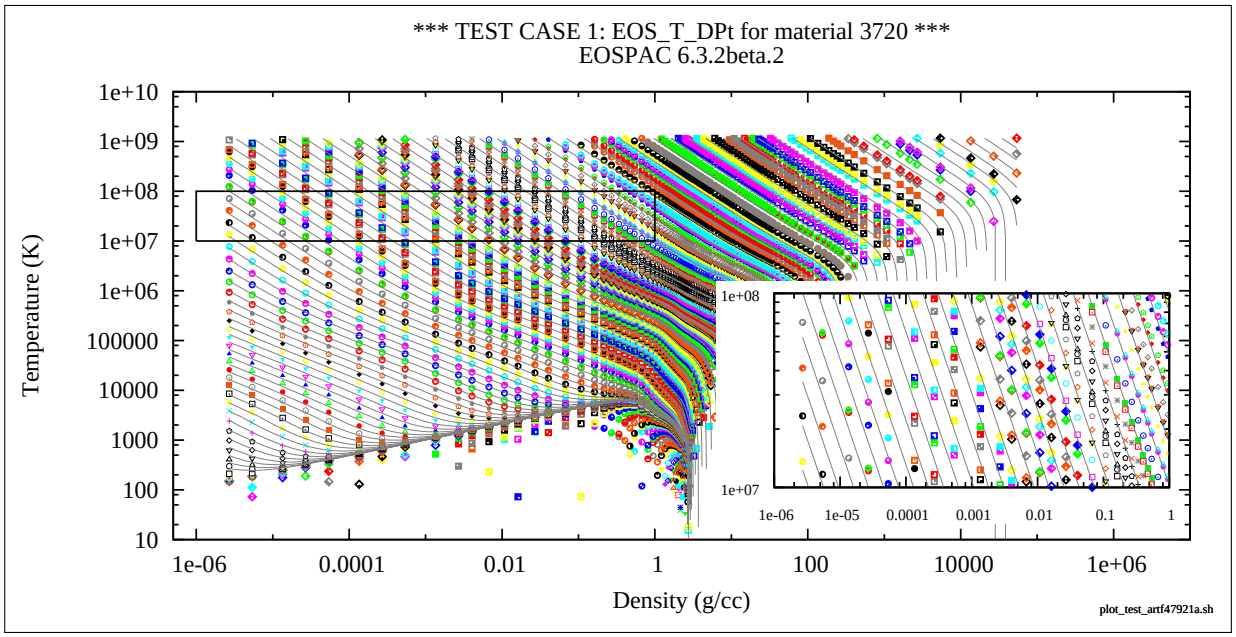

Figure 6: Interpolated $T(\rho, Pt)$ isobars (gray curves), which were calculated using EOSPAC 6's default inverse interpolation mode, superimposed on the representative SESAME data.

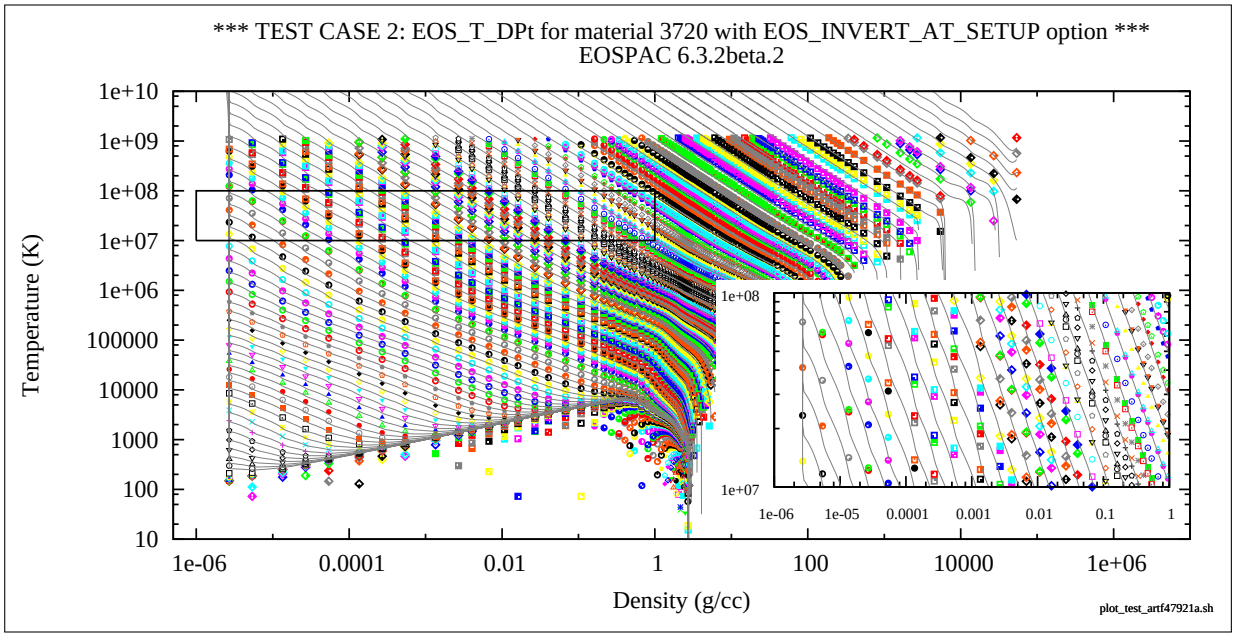

Figure 7: Interpolated $T(\rho, Pt)$ isobars (gray curves), which were calculated using EOSPAC 6's pre-inverted (i.e., *EOS_INVERT_AT_SETUP*) inverse interpolation mode, superimposed on the representative SESAME data.

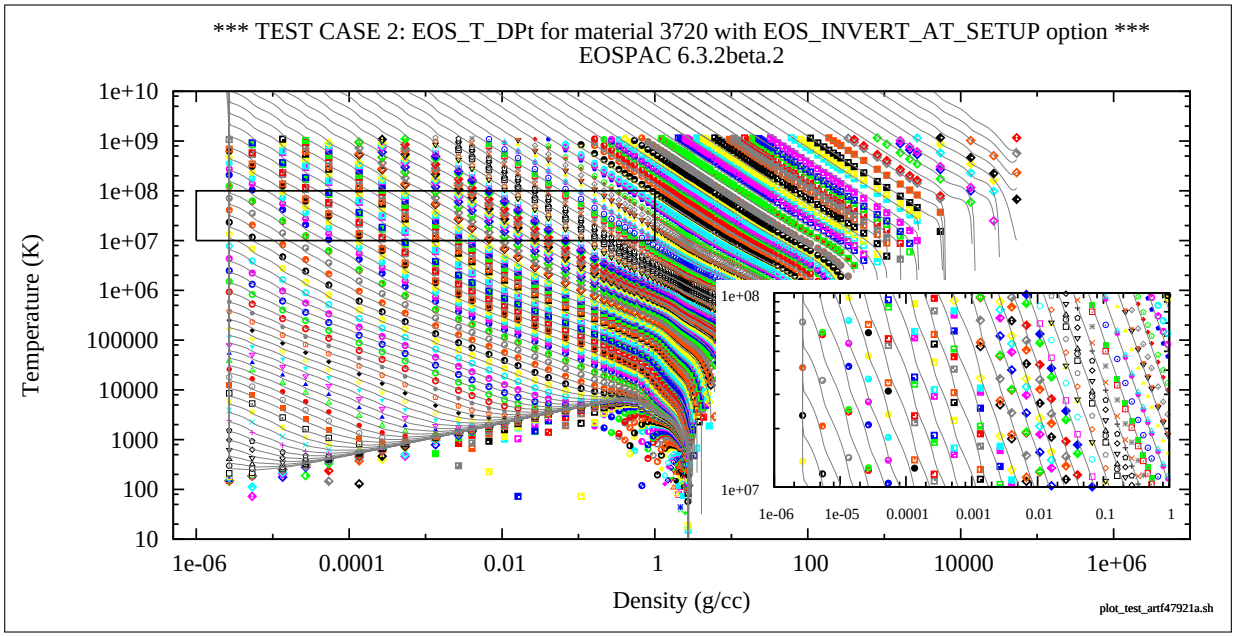

Figure 8: Interpolated $T(\rho, Pt)$ isobars (gray curves), which were calculated using EOSPAC 6's pre-inverted (i.e., *EOS_INVERT_AT_SETUP*) inverse interpolation mode and the EOS_INSERT_DATA option with a value of one, superimposed on the representative SESAME data.

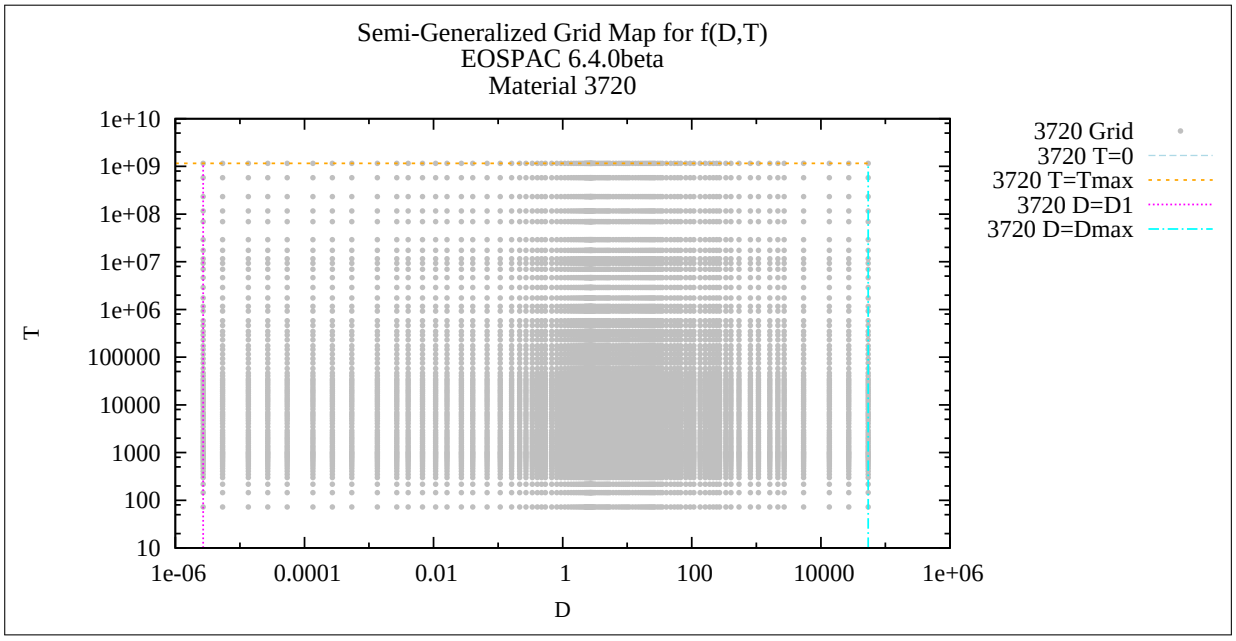

Figure 9: Rectangular SESAME grid of density (D) and temperature (T).

B. Naïve Solution

It was initially considered that the preexisting EOSPAC 6 option named EOS_INSERT_DATA[2] could be used to mitigate the pathological inverse interpolation results; however, this improvement is not always guaranteed as shown in figure 8 (page 7). Using the EOS_INSERT_DATA option imposes additional memory requirements to store the pre-inverted tables(s) that is likely not worth the lack of a guaranteed improvement of the pre-inverted interpolation mode's numerical results.

C. Non-rectangular Grids

It is useful to pause here so that a review of the general table inversion process can be made. The SESAME data is stored with an irregularly-spaced rectangular grid of density (ρ) and temperature (T) – see figure 9 (page 8) for a representation of the (ρ,T) grid of the SESAME data used herein. When a SESAME table is inverted[3], the resulting inverted table is forced to be stored in a similarly-rectangular fashion; however, the valid independent variable ranges of the newly-inverted table excludes all extrapolated values, which results in a valid grid that is not rectangular. Figures 10 to 12 (pages 9 and 10) show representations of the varied inverted grids of the SESAME data used in this assessment.

The irregular relative spacing of the inverted grids has been determined as the cause of the interpolation pathologies described herein. Essentially, the Rational Interpolator [5], which was designed to be well-suited for interpolation on sparse grids with logarithmic spacing (i.e., SESAME data), is sensitive to such grid

[2]The EOS_INSERT_DATA option causes EOSPAC 6 to insert grid points between each original grid point with respect to all independent variables (i.e., increase grid resolution). The value of the eos_SetOption parameter, tableOptionVal, is to contain the user-defined number of data points to insert between existing data points. This option causes the table, which is stored in memory, to be $(kM-1)(kN-1)$ where k is the aforementioned user-defined number, and M and N collectively define the grid size of the original SESAME table. [1, p. D-3]

[3]Table inversion a transformation exchanging the dependent variable with one of the independent variable(s). See section B. for further discussion.

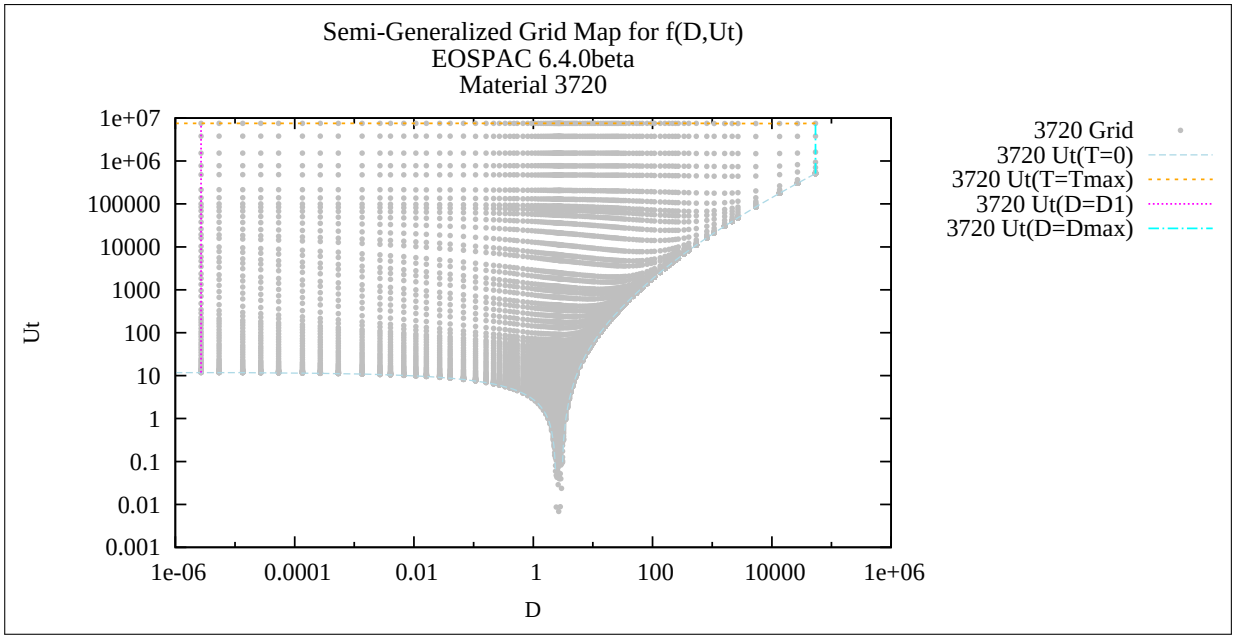

Figure 10: Non-rectangular SESAME grid of density (D) and internal energy (Ut).

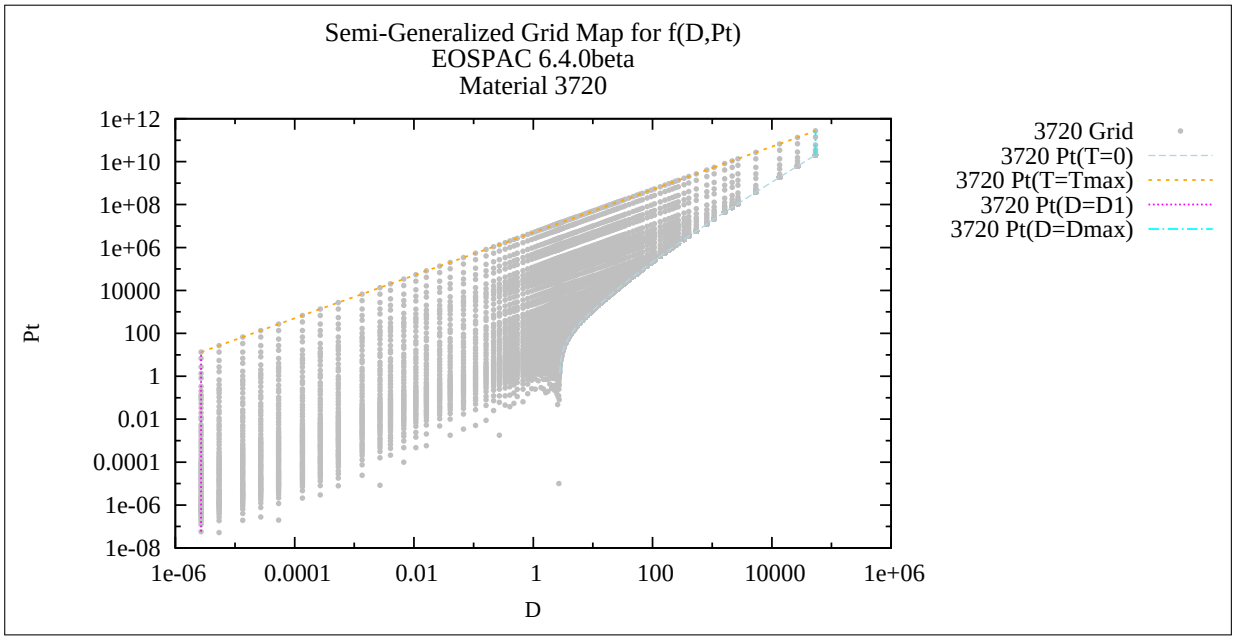

Figure 11: Non-rectangular SESAME grid of density (D) and pressure (Pt).

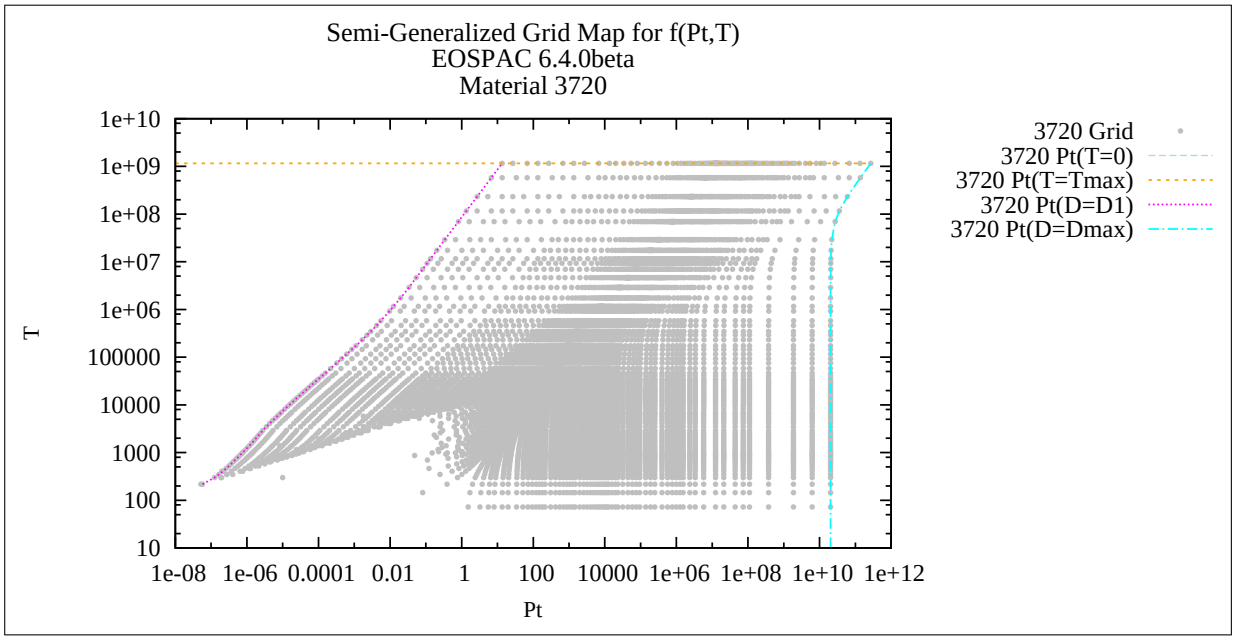

Figure 12: Non-rectangular SESAME grid of pressure (Pt) and temperature (T).

irregularities.

D. Chosen Solution

Historical versions of EOSPAC [7][8] used the following data transforms to create the grids of varied inverted tables:

$$U^*(\rho, T) = Ut(\rho, T) - Uc(\rho) \tag{1}$$

$$P^*(\rho, T) = \frac{Pt(\rho, T) - Pc(\rho)}{\rho} \tag{2}$$

In addition to those historical transforms, EOSPAC 6 now eliminates the isochore at $\rho = 0$ prior to table inversion, because it causes $P^*(\rho, T) \to \infty$ and it is not a physically-meaningful state of matter.

One can easily recognize that the transforms defined by equations (1) and (2), eliminate much of the dynamic range of the both Ut and Pt by subtracting their associated cold curve data. Additionally, it is apparent from the ideal gas law that internal energy is directly proportional to temperature. Where $v = 1/\rho$, the differential for internal energy is dependent upon (v, T)

$$dU = \left(\frac{\partial U}{\partial T}\right)_v TdT + \left(\frac{\partial U}{\partial v}\right)_T Tdv \tag{3}$$

One of the important features of an ideal gas is that its internal energy depends only upon its temperature, so equation (3) becomes

$$dU = \left(\frac{\partial U}{\partial T}\right)_v TdT \tag{4}$$

From equations (1) and (4), it is concluded that

$$U^* \propto T \tag{5}$$

Similarly, the ideal gas law states that the ratio of pressure and density is directly proportional to temperature:

$$Pv = RT \tag{6}$$

The R of equation (6) is the Universal Gas Constant.
Given $v = 1/\rho$, equation (6) can be rewritten as

$$\frac{P}{\rho} = RT \tag{7}$$

From equations (2) and (7), it is concluded that

$$P^* \propto T \tag{8}$$

Given the fact that SESAME data is tabulated with density and temperature as independent variables, it is reasonable to conclude that the transforms of equations (1) and (2) create data that are "temperature-like" quantities, and the non-rectangular grids represented in figures 10 to 12 are transformed into rectangular grid of density (ρ) and a "temperature-like" quantity like the representation in figure 9.

IV. Results

The chosen solution described above (section D.) details the data transformations that are now performed by EOSPAC 6 when an inverted table is generated and stored in memory as a result of using the *EOS_INVERT_AT_SETUP* option during the setup phase of operation. When the new EOSPAC 6 setup algorithms are applied, the interpolated results shown in figures 4 and 5, which are based upon the EOS trajectories shown in figure 1, are corrected to those in figures 13 and 14 (page 12). This observed correction is concluded to be the result of the both imposed grid regularity of the inverse data tabulation and the shift of the trajectory from the tabulated "edge" of the inverted data table.

A. Numerical Consistency

A question concerning the consistency between the two modes of inverse interpolations remained: "How good are the inverted interpolation results of the corrected pre-inverted mode?" To answer the question, several comparisons were made that identified the distributions of relative differences between the interpolation results of the default mode and the invert-at-setup mode. Very large samplings of inputs for the EOS_T_DPt, EOS_T_DUt, EOS_Ut_DPt, EOS_Pt_DUt, and EOS_D_PtT tables were used to calculate the relative differences of the interpolation results as shown in figures 15 to 19 (pages 13 to 15). Note that the vast majority of the interpolated results are within one percent of EOSPAC 6's default mode of interpolation for all inverted domains except the *(Pt,T)* domain shown in figure 19.

A follow-up question was then asked, "Can this numerical agreement be improved?" The option named EOS_INSERT_DATA [1, p. D-3] was employed in an attempt to answer the second question. Figures 20 to 22 (pages 15 and 16) demonstrate significantly-improved numerical agreement for the repeated interpolation result comparisons of figure 19 with the additional usage of the EOS_INSERT_DATA option and corresponding option values of one through three respectively.

Tables 3 to 7 list statistical information for the various inverse interpolation tests when compared to the baseline interpolation results, which were obtained using EOSPAC 6's default interpolation mode. In

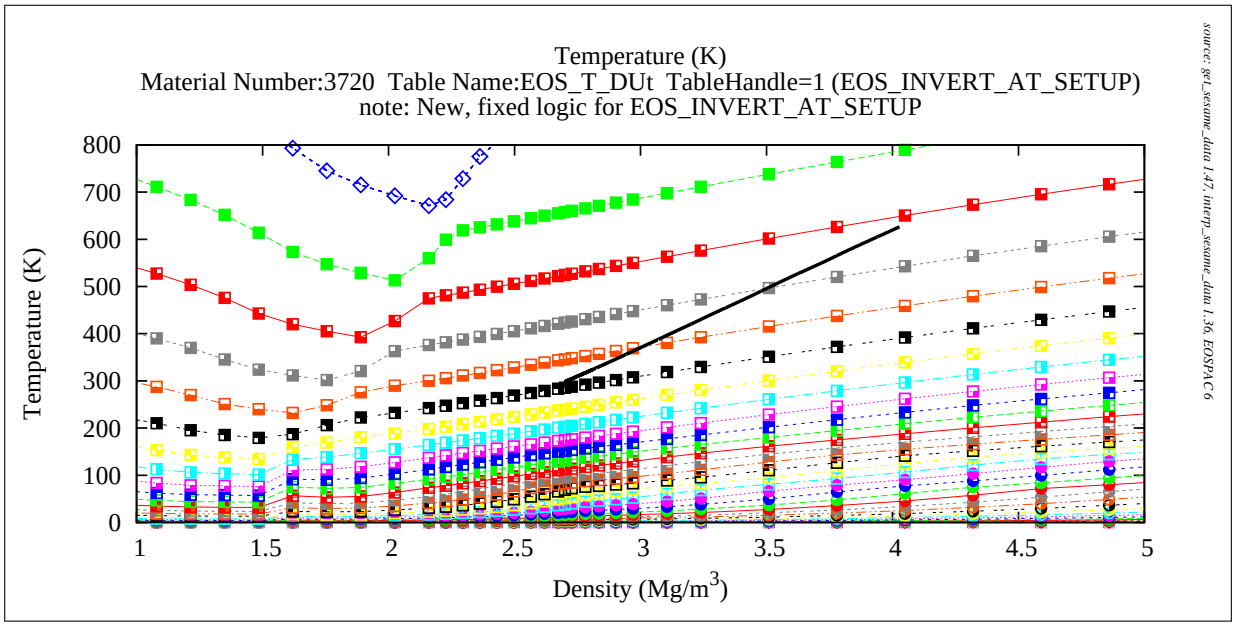

Figure 13: Correct interpolated $T(\rho, Ut)$ trajectory (black curve), which was calculated using EOSPAC 6's pre-inverted (i.e., *EOS_INVERT_AT_SETUP*) inverse interpolation mode, superimposed on the representative transformed iso-energy lines of SESAME data.

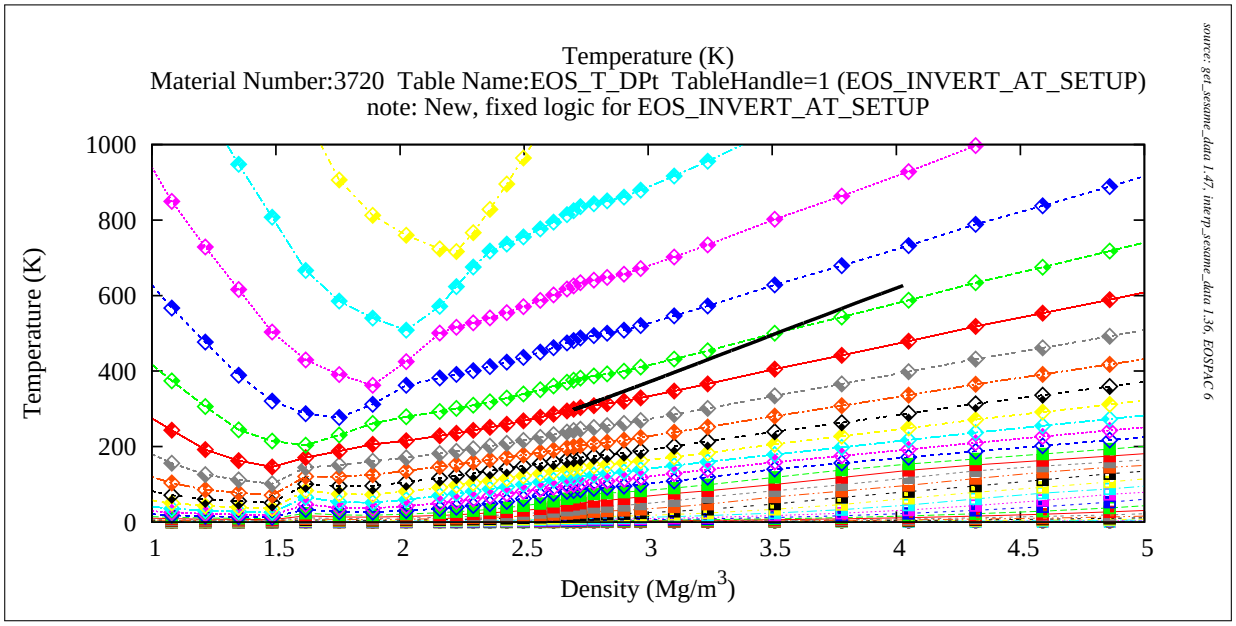

Figure 14: Correct interpolated $T(\rho, Pt)$ trajectory (black curve), which was calculated using EOSPAC 6's pre-inverted (i.e., *EOS_INVERT_AT_SETUP*) inverse interpolation mode, superimposed on the representative transformed isobaric lines of SESAME data.

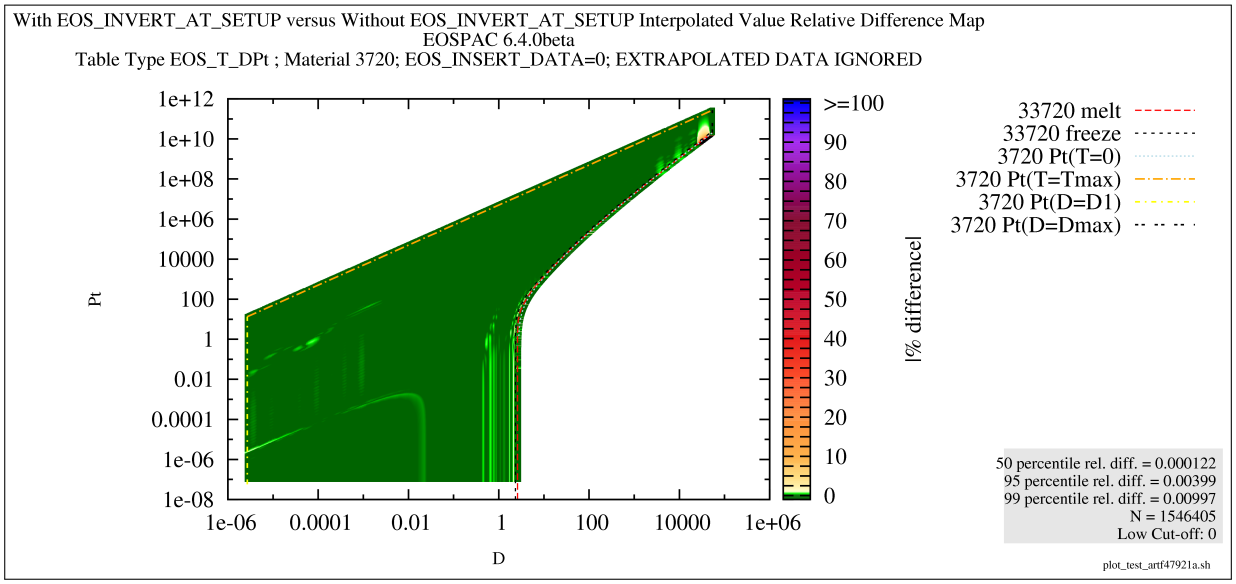

Figure 15: Color map of relative differences comparing the interpolation of $T(\rho, Pt)$, which was calculated using both of EOSPAC 6's default and pre-inverted (i.e., *EOS_INVERT_AT_SETUP*) inverse interpolation modes.

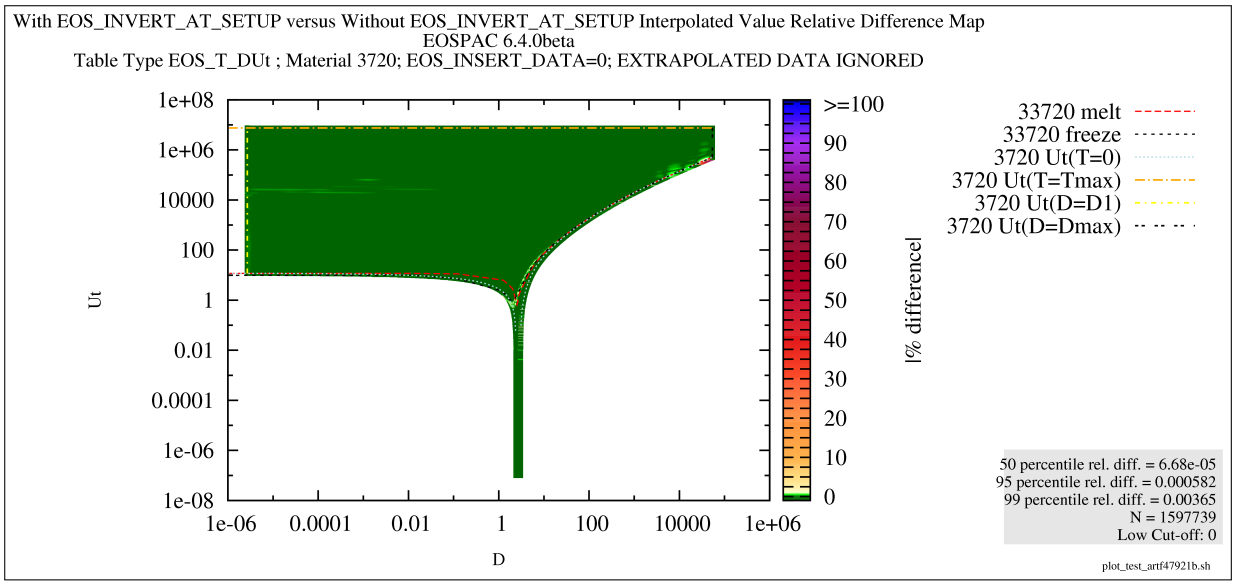

Figure 16: Color map of relative differences comparing the interpolation of $T(\rho, Ut)$, which was calculated using both of EOSPAC 6's default and pre-inverted (i.e., *EOS_INVERT_AT_SETUP*) inverse interpolation modes.

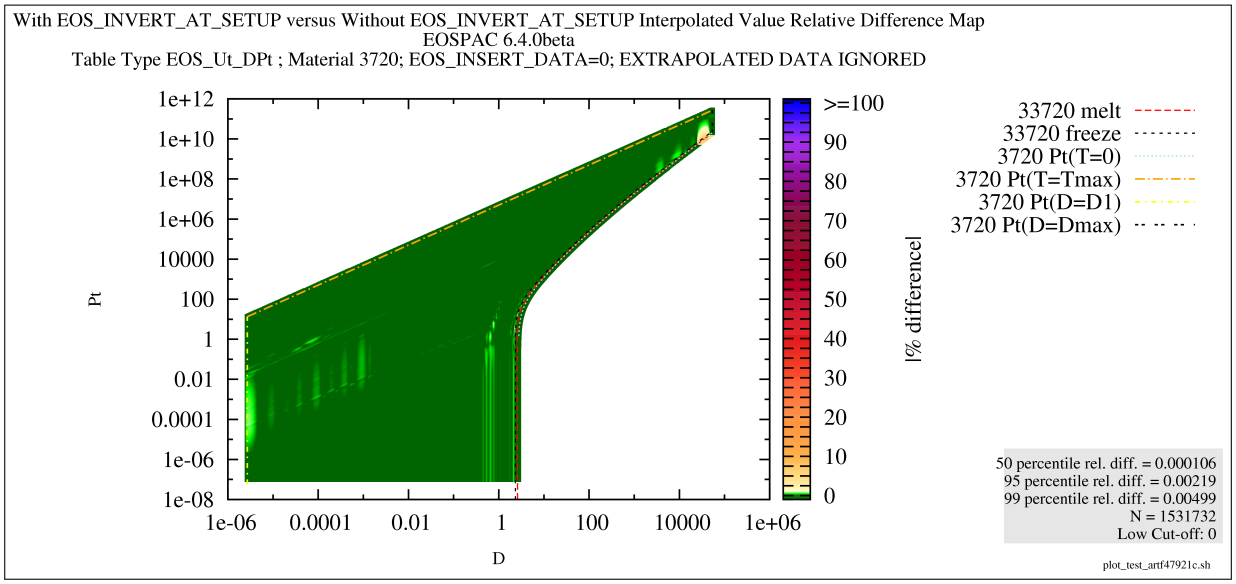

Figure 17: Color map of relative differences comparing the interpolation of $Ut(\rho, Pt)$, which was calculated using both of EOSPAC 6's default and pre-inverted (i.e., *EOS_INVERT_AT_SETUP*) inverse interpolation modes.

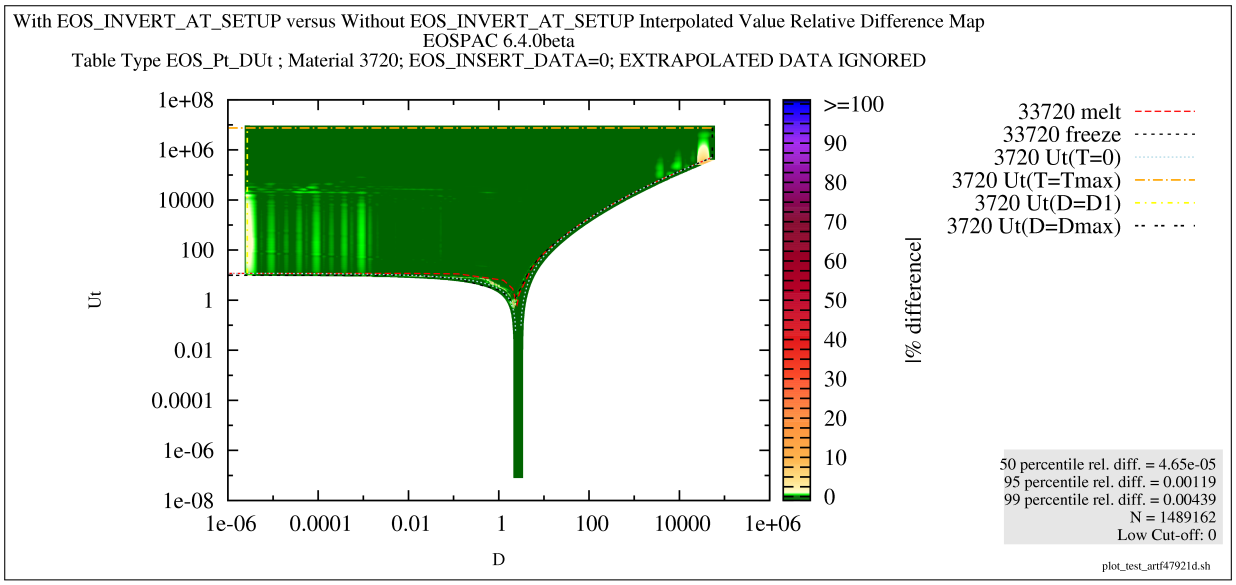

Figure 18: Color map of relative differences comparing the interpolation of $Pt(\rho, Ut)$, which was calculated using both of EOSPAC 6's default and pre-inverted (i.e., *EOS_INVERT_AT_SETUP*) inverse interpolation modes.

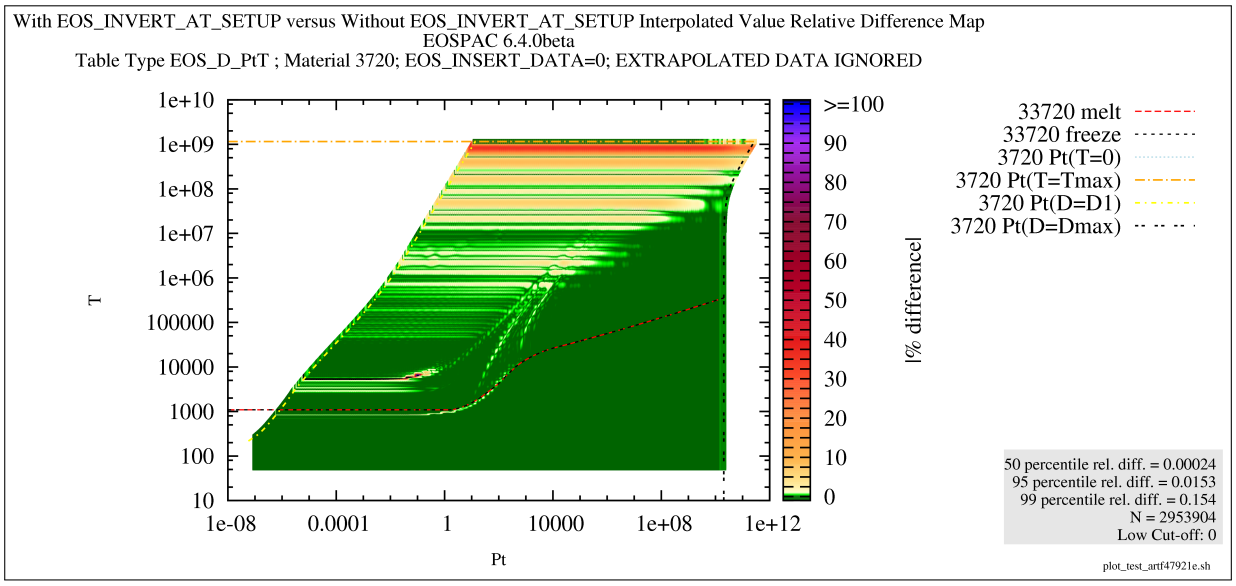

Figure 19: Color map of relative differences comparing the interpolation of $\rho(Pt, T)$, which was calculated using both of EOSPAC 6's default and pre-inverted (i.e., *EOS_INVERT_AT_SETUP*) inverse interpolation modes.

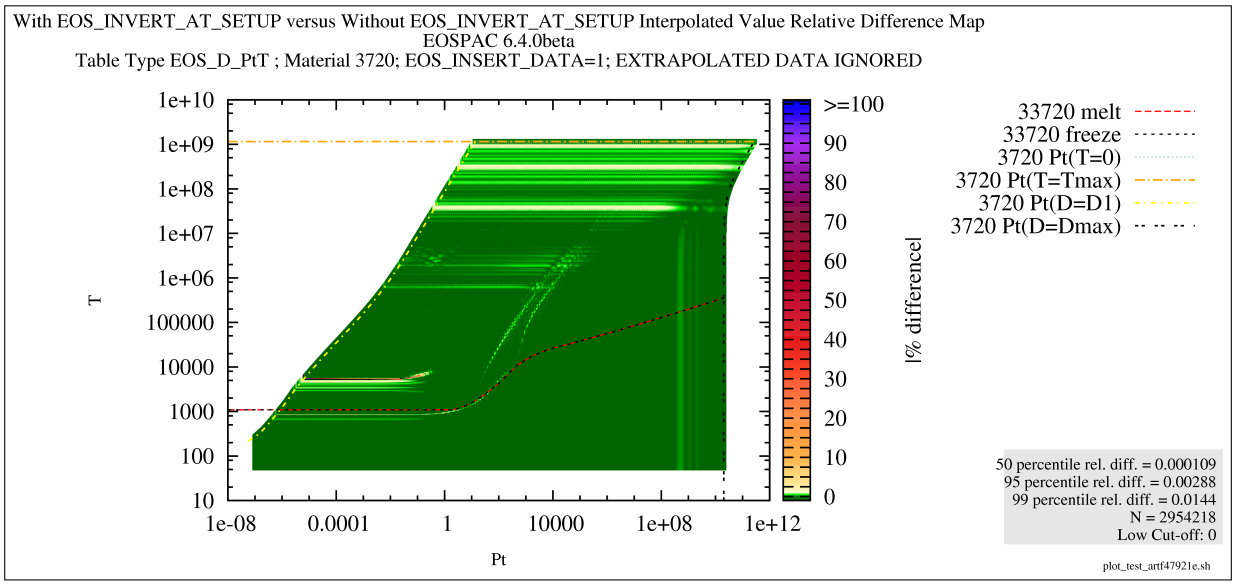

Figure 20: Color map of relative differences comparing the interpolation of $\rho(Pt, T)$, which was calculated using both of EOSPAC 6's default and pre-inverted (i.e., *EOS_INVERT_AT_SETUP*) inverse interpolation modes and the *EOS_INSERT_DATA=1* option enabled.

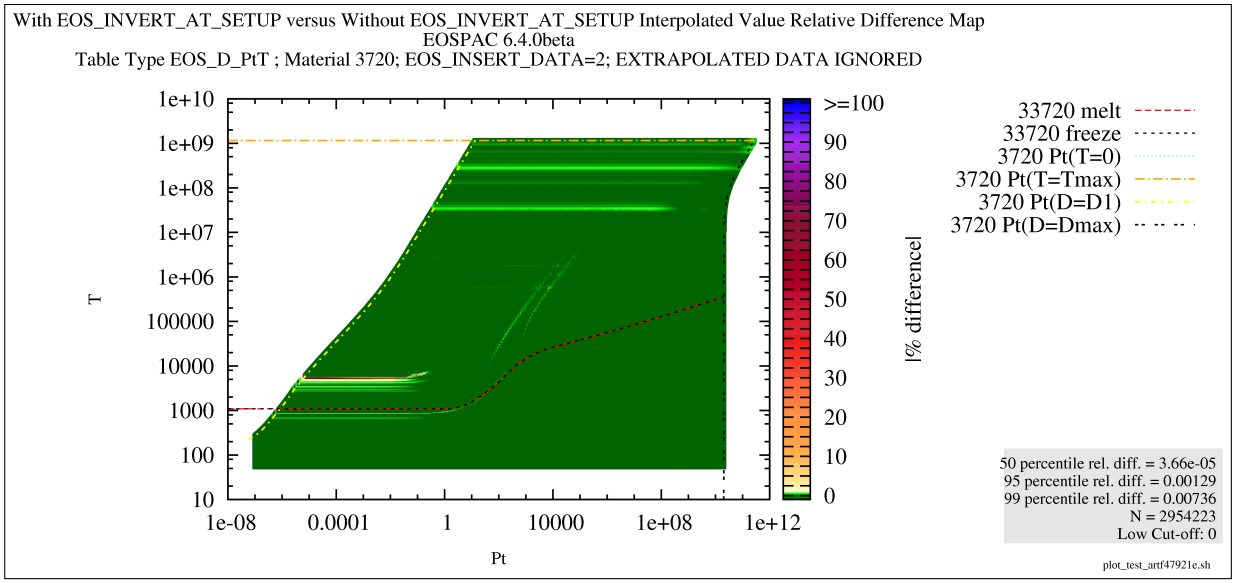

Figure 21: Color map of relative differences comparing the interpolation of $\rho(Pt, T)$, which was calculated using both of EOSPAC 6's default and pre-inverted (i.e., *EOS_INVERT_AT_SETUP*) inverse interpolation modes and the *EOS_INSERT_DATA=2* option enabled.

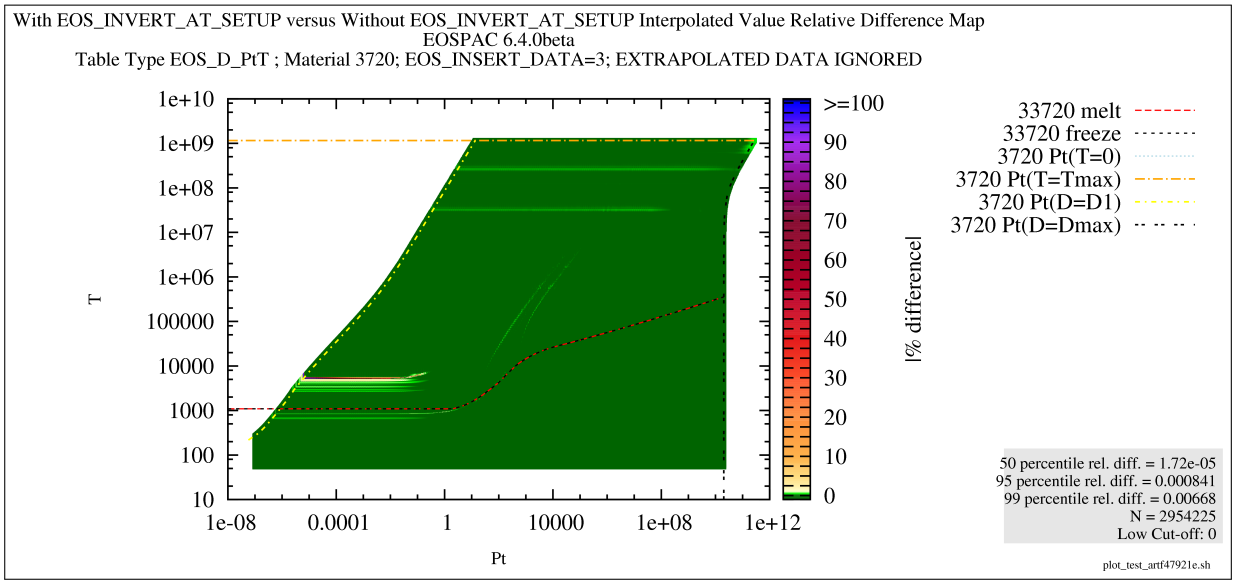

Figure 22: Color map of relative differences comparing the interpolation of $\rho(Pt, T)$, which was calculated using both of EOSPAC 6's default and pre-inverted (i.e., *EOS_INVERT_AT_SETUP*) inverse interpolation modes and the *EOS_INSERT_DATA=3* option enabled.

all of the tables 3 to 7, the test 1 interpolation results are used as the aforementioned baseline. Tests 2 - 5 each used the pre-inverted interpolation mode and varying values associated with the EOS_INSERT_DATA option. Note that the relative agreement is good, and it improves with increasing values associated with the EOS_INSERT_DATA option – particularly for the EOS_D_PtT table type summarized in table 7.

Table 3: $T(\rho, Pt)$ statistics summary of the EOS_T_DPt interpolation relative differences, with respect to TEST NO. 1.

		RELATIVE DIFFERENCE			
TEST NO.	N	MEDIAN	$95^{th}\% - ILE$	$99^{th}\% - ILE$	INVERT-AT-SETUP
1	-	-	-	-	no
2	1546405	0.000121862	0.00398505	0.00997051	yes
3	1546404	8.6294e-05	0.00166031	0.00632026	yes (insert 1)
4	1546403	3.47622e-05	0.000767908	0.00442053	yes (insert 2)
5	1546403	1.44036e-05	0.000400697	0.00153078	yes (insert 3)

Table 4: $T(\rho, Ut)$ statistics summary of the EOS_T_DUt interpolation relative differences, with respect to TEST NO. 1.

		RELATIVE DIFFERENCE			
TEST NO.	N	MEDIAN	$95^{th}\% - ILE$	$99^{th}\% - ILE$	INVERT-AT-SETUP
1	-	-	-	-	no
2	1597739	6.67667e-05	0.00058225	0.00364641	yes
3	1597731	6.64696e-05	0.000731147	0.00277559	yes (insert 1)
4	1597733	2.38603e-05	0.000305577	0.00121687	yes (insert 2)
5	1597733	1.01629e-05	0.00016802	0.000729068	yes (insert 3)

Table 5: $T(\rho, Pt)$ statistics summary of the EOS_Ut_DPt interpolation relative differences, with respect to TEST NO. 1.

		RELATIVE DIFFERENCE			
TEST NO.	N	MEDIAN	$95^{th}\% - ILE$	$99^{th}\% - ILE$	INVERT-AT-SETUP
1	-	-	-	-	no
2	1531732	0.000106173	0.00219108	0.00499237	yes
3	1531722	9.63695e-05	0.00132514	0.00352057	yes (insert 1)
4	1531725	3.75878e-05	0.000469033	0.00213833	yes (insert 2)
5	1531729	1.69544e-05	0.000244718	0.000762062	yes (insert 3)

Table 6: $T(\rho, Ut)$ statistics summary of the EOS_Pt_DUt interpolation relative differences, with respect to TEST NO. 1.

		RELATIVE DIFFERENCE			
TEST NO.	N	MEDIAN	$95^{th}\% - ILE$	$99^{th}\% - ILE$	INVERT-AT-SETUP
1	-	-	-	-	no

Continued on next page

Table 6: $T(\rho, Ut)$ statistics summary of the EOS_Pt_DUt interpolation relative differences, with respect to TEST NO. 1. *Continued from previous page.*

		RELATIVE DIFFERENCE			
TEST NO.	N	MEDIAN	$95^{th}\% - ILE$	$99^{th}\% - ILE$	INVERT-AT-SETUP
2	1489162	4.64746e-05	0.00119407	0.00439156	yes
3	1489164	4.54598e-05	0.000731815	0.00206801	yes (insert 1)
4	1489165	1.56583e-05	0.000334224	0.00104273	yes (insert 2)
5	1489163	6.94408e-06	0.000178797	0.000618875	yes (insert 3)

Table 7: $\rho(Pt, T)$ statistics summary of the EOS_D_PtT interpolation relative differences, with respect to TEST NO. 1.

		RELATIVE DIFFERENCE			
TEST NO.	N	MEDIAN	$95^{th}\% - ILE$	$99^{th}\% - ILE$	INVERT-AT-SETUP
1	-	-	-	-	no
2	2953904	0.000240012	0.015265	0.15387	yes
3	2954218	0.000109216	0.00288377	0.0143757	yes (insert 1)
4	2954223	3.66207e-05	0.00128999	0.00735584	yes (insert 2)
5	2954225	1.72121e-05	0.00084115	0.00668069	yes (insert 3)

B. Performance

Tables 8 to 12 list timing results for the various inverse interpolation tests that use either EOSPAC 6's default inverse interpolation mode or EOSPAC 6's pre-inverted inverse interpolation mode. In all of tables 8 to 12, test 1 shows the total CPU times for setup and interpolation using the default interpolation mode. The remaining CPU timing results are shown for the pre-inverted interpolation mode and varying values associated with the EOS_INSERT_DATA option. In this collection of analyses, the pre-inverted interpolation mode is demonstrated to provide a factor of 10 to 24 speed-up as compared to the default interpolation mode.

Table 8: $T(\rho, Pt)$ interpolation performance summary for EOS_T_DPt.

	CPUCYCLES			
TEST NO.	SETUP	INTERPOLATE	SPEED-UP	INVERT-AT-SETUP
1	134	16739	-	no
2	40	731	x23	yes
3	280	758	x22	yes (insert 1)
4	618	734	x23	yes (insert 2)
5	909	725	x23	yes (insert 3)

Table 9: $T(\rho, Ut)$ interpolation performance summary for EOS_T_DUt.

	CPUCYCLES			
TEST NO.	SETUP	INTERPOLATE	SPEED-UP	INVERT-AT-SETUP
1	45	7466	-	no
2	30	706	x11	yes
3	89	703	x11	yes (insert 1)
4	252	755	x10	yes (insert 2)
5	372	732	x10	yes (insert 3)

Table 10: $Ut(\rho, Ut)$ interpolation performance summary for EOS_Ut_DPt.

	CPUCYCLES			
TEST NO.	SETUP	INTERPOLATE	SPEED-UP	INVERT-AT-SETUP
1	139	17323	-	no
2	184	763	x23	yes
3	253	738	x23	yes (insert 1)
4	724	736	x24	yes (insert 2)
5	988	713	x24	yes (insert 3)

Table 11: $Pt(\rho, Ut)$ interpolation performance summary for EOS_Pt_DUt.

	CPUCYCLES			
TEST NO.	SETUP	INTERPOLATE	SPEED-UP	INVERT-AT-SETUP
1	42	8266	-	no
2	32	723	x11	yes
3	96	719	x11	yes (insert 1)
4	255	728	x11	yes (insert 2)
5	393	732	x11	yes (insert 3)

Table 12: $\rho(Pt, T)$ interpolation performance summary for EOS_D_PtT.

	CPUCYCLES			
TEST NO.	SETUP	INTERPOLATE	SPEED-UP	INVERT-AT-SETUP
1	35	14161	-	no
2	35	633	x22	yes
3	94	616	x23	yes (insert 1)
4	424	614	x23	yes (insert 2)
5	627	609	x23	yes (insert 3)

V. Conclusions

In spite of the problem resolutions advertised with the release of version 6.3.2beta.2, significant interpolation pathologies were discovered to occur when EOSPAC 6's host software enabled pre-inversion with the *EOS_INVERT_AT_SETUP* option. This document describes a solution that uses data transformations found in EOSPAC 5 and its predecessors. The numerical results and performance characteristics of both the default and pre-inverted interpolation modes in both EOSPAC 6.3.2beta.2 and the fixed logic of EOSPAC 6.4.0beta.1 were presented, and the latter software release was shown to produce significantly-improved numerical results for the pre-inverted interpolation mode.

VI. References

[1] David A. Pimentel, *(U) EOSPAC User's Manual: Version 6.3, Revision 4*, Los Alamos National Laboratory report LA-UR-14-29289 (September 20, 2016).

[2] S. P. Lyon and J. D. Johnson, *SESAME: The Los Alamos National Laboratory Equation Of State Database*, Los Alamos National Laboratory report LA-UR-92-3407 (1992).

[3] David A. Pimentel, *(U) EOSPAC 6 interpolation performance assessment*, Los Alamos National Laboratory memorandum XCP-5:15-027(U) (March 30, 2015).

[4] David A. Pimentel, *(U) EOSPAC 6 interpolation performance assessment, parte dois*, Los Alamos National Laboratory memorandum XCP-5:17-006(U) (November 15, 2016).

[5] G. I. Kerley (Gerald I.), *Rational function method of interpolation*, Los Alamos Scientific Laboratory report LA-6903-MS (August 1977).

[6] Scott D. Crockett, *Analysis of Sesame 3720, A New Aluminum Equation State*, Los Alamos National Laboratory report LA-UR-04-6442, (September 10, 2004).

[7] C. W. Cranfill, *EOSPAC: A Subroutine Package For Accessing The Los Alamos Sesame EOS Data Library*, Los Alamos National Laboratory report LA-09728-MS (March 10, 1983).

[8] David A. Pimentel, *EOSPAC 5 Users Manual*, Los Alamos National Laboratory report LA-UR-03-4510, (July 2, 2003).